We are IntechOpen, the world's leading publisher of Open Access books Built by scientists, for scientists

4,800
Open access books available

122,000
International authors and editors

135M
Downloads

Our authors are among the

154
Countries delivered to

TOP 1%
most cited scientists

12.2%
Contributors from top 500 universities

WEB OF SCIENCE™

Selection of our books indexed in the Book Citation Index in Web of Science™ Core Collection (BKCI)

Interested in publishing with us?
Contact book.department@intechopen.com

Numbers displayed above are based on latest data collected.
For more information visit www.intechopen.com

4

Mutations in the CP43 Protein of Photosystem II Affect PSII Function and Cytochrome C_{550} Binding

Brandon D. Burch[1], Terry M. Bricker[2] and Cindy Putnam-Evans[1]
[1]*East Carolina University/Biology Department*
[2]*Louisiana State University/Department of Biological Sciences*
USA

1. Introduction

During the process of photosynthesis, light energy is converted to chemical energy that is utilized in the biosynthesis of carbohydrate. The initial events of photosynthesis in cyanobacteria, green algae and higher plants are the photoinduced transfer of electrons from water to plastoquinone. These reactions are catalyzed by Photosystem II (PSII), a large pigment-protein complex embedded within the thylakoid membrane (Renger, et al., 2008). The reactions catalyzed by PSII proceed as follows. First, light is trapped by pigments, predominately chlorophyll, associated with the thylakoid membrane (Glazer, 1983). Excitation energy is then transferred to the photochemically active chlorophyll species P_{680}. Excited P_{680} then donates an electron (charge separation) to the primary PSII electron acceptor, a protein-bound pheophytin molecule (Klimov et al., 1980). Pheophytin is then oxidized by a tightly bound plastoquinone, Q_A, which in turn reduces a loosely bound plastoquinone, Q_B. A second light-induced charge separation results in the formation of plastoquinol (Q_BH_2). Photooxidized P_{680} is reduced by the primary donor of PSII, a tyrosyl radical ($Y_Z^{\bullet}$) that is Tyr161 of the D1 protein of PSII (Debus et al., 1988a; Debus et al., 1988b). Y_Z then is reduced by an electron from the oxygen-evolving complex of PSII, located on the lumenal face of the thylakoid. The catalytic site of the oxygen-evolving complex consists of a metal ion cluster of four manganese atoms and one calcium atom bound via five μ-oxo-bridges (Mn_4CaO_5 cluster; Umena et al., 2011). Two chloride ions bound nearby are also required for activity. The oxygen-evolving complex functions to extract electrons and protons from water, ultimately resulting in the release of molecular oxygen. The manganese atoms cycle through a series of redox states, or S states (Joliot et al., 1969; Kok et al., 1970), from S_0 to S_4, with each S state representing a successively more oxidized form of the cluster. One molecule of O_2 is evolved when four electrons and four protons are extracted by the Mn_4CaO_5 cluster.

PSII consists of both intrinsic thylakoid polypeptides and extrinsic polypeptides located within the thylakoid lumen. Together, these proteins ligate the Mn_4CaO_5 cluster, chlorophylls and other pigments, and the electron transport chain components. The intrinsic polypeptides necessary to form a PSII complex capable of evolving oxygen are CP47, CP43, D1, D2, the α and β subunits of cytochrome b_{559}, and the 4kDa *psb*I gene product (Bricker et

al., 2011). In higher plants, three extrinsic proteins, PsbO (previously termed the manganese-stabilizing protein), PsbP and PsbQ, are required for maximal rates of oxygen evolution under physiological conditions (Bricker, 1992). In cyanobacteria, cytochrome c_{550} and a 12 kDa protein (PsbU) perform similar functions to PsbP and PsbQ. However, cyanobacteria also contain homologues of the higher plant PsbP and PsbQ proteins, though their roles are not well defined (Roose et al., 2007). In the absence of these extrinsic proteins, PSII complexes retain the ability to evolve oxygen, but at significantly reduced rates. This ability to evolve oxygen is dependent upon the presence of high, non-physiological, concentrations of calcium and chloride. The extrinsic proteins appear to act as a diffusional barrier that sequesters chloride and calcium in the vicinity of the oxygen-evolving complex (Bricker et al., 2011). They also act to protect the Mn_4CaO_5 cluster from exogenous reductants (Ghanotakis et al., 1984).

CP43 is an integral thylakoid protein. CP43 binds 13 chlorophyll molecules and is a component of the proximal antenna of PSII. X-ray analysis of PS II from *Thermosynechococcus elongatus* and *Thermosynechococcus vulcanus* shows that CP43 contains six transmembrane alpha helices and five hydrophilic loops that connect the membrane-spanning domains (Zouni et al., 2001; Kamiya & Shen, 2003; Ferreira et al., 2004; Umena et al., 2011). One of these loops, the large extrinsic loop E, spans amino acid residues ^{278}Asn-^{410}Trp and is located between the fifth and sixth membrane-spanning helices. The large extrinsic loop is exposed to the lumenal side of the thylakoid membrane and lies close to all three of the extrinsic PSII proteins as well as the Mn_4CaO_5 cluster. We previously constructed and extensively characterized the R320S (R305S in our original numbering scheme[1]) mutant in the large extrinsic loop E of CP43 in the cyanobacterium *Synechocystis* 6803, and showed that it has impaired PSII activity under chloride-limiting conditions (Knoepfle et al., 1999; Young et al., 2002). Isolated PSII from this mutant failed to bind the extrinsic PSII protein, cytochrome c_{550} (Bricker et al., 2002).

In this chapter, we will briefly review the role of both chloride and the CP43 large extrinsic loop E in the water-oxidizing process, and present new data on the characterization of additional mutations within the large extrinsic loop E that provide information about the nature of interaction of CP43 with the extrinsic PSII proteins. These data will be discussed within the context of the most current x-ray structure of PSII.

2. Structure of the Mn_4CaO_5 cluster

The structure of the manganese cluster has been the focus of intense study. Early x-ray structures obtained at low to medium resolution were known to be affected by radiation damage, which alters the valence state of the manganese and also potentially alters the ligand field (Grabolle et al., 2006). Nonetheless, these structures provided the first data on the positions of the protein subunits, chlorophylls and other cofactors. However, they did not allow for a highly refined, detailed structure of the manganese cluster. The manganese cluster models were proposed relying on interatomic distances derived from EXAFS experiments (Dau et al., 2008). The recent x-ray structure at 1.9 Å from *Thermosynechococcus*

[1] Due to differences in initiation sites, the CP43 proteins from various cyanobacteria are of varying lengths. In this article, unless otherwise specified, we will follow the common practice of numbering the amino acids using the corresponding numbering in *Thermosynechococcus vulcanus*, the strain from which the latest x-ray structure was derived.

vulcanus provided a well-resolved, detailed structure of the 4 manganese, calcium, and two chloride atoms, as well as revealing the positions of potential substrate water molecules, thus paving the way for an understanding of the mechanistic aspects of water oxidation (Umena et al., 2011).

The Mn_4CaO_5 cluster has a distorted, chair-like structure in which three of the manganese (Mn1, Mn2, Mn3) and the calcium atom form a distorted cubane-like structure (see Fig. 1). The fourth manganese atom (Mn4), the so-called "dangler" manganese, lies outside of the cubane. Mn1, Mn2 and Mn3 and the calcium atom are linked via four oxygen atoms (μ–oxo bridges). Mn4 is linked by a fifth oxygen to Mn1 and Mn3. In fact, each two adjacent manganese atoms are linked by a di-μ-oxo bridge and the calcium atom is linked to all four manganese via oxo bridges. Four water molecules were observed in the x-ray structure in close proximity to the Mn_4CaO_5 cluster. Two of these appear to be associated with Mn4 and the other two with the calcium atom. It has been speculated that least one of these is a substrate for the water oxidizing reaction. Two chloride ions were also revealed in the structure. These flank the cluster and are not bound directly to the manganese or calcium atoms, but rather are ligated via two amino acids and two water molecules each. For each of these chloride ions, bound indirectly to the Mn_4CaO_5 cluster, one ligand is contributed by the backbone nitrogen of a glutamate residue.

In addition to the metal atoms and water, the protein ligands for the Mn_4CaO_5 cluster were identified. While most of the ligands are contributed by the D1 protein, CP43 contributes one bi-dentate ligand to the cluster, Glu354. Glu354 ligates both Mn2 and Mn3. What is additionally interesting is that this glutamate residue binds one of the chloride ions flanking the cluster. The other chloride ion is bound by Glu333 of the D1 protein. Glu333 is a bi-dentate ligand to Mn3 and Mn4. It has been proposed that the chloride ions help to maintain the structural integrity of the Mn_4CaO_5 cluster by maintaining the stable coordination of these glutamate residues to manganese (Umena et al., 2011; Kawakami et al., 2011). Also, the chloride ions lie at the beginning of two putative proton and/or water exit channels. Chloride may also play a role in stabilizing these channels.

3. Role of chloride in oxygen evolution

Chloride is required for both the assembly and the stability of the oxygen-evolving complex and is sequestered at the active site by the PSII extrinsic proteins. Chloride depletion of isolated PSII preparations has profound effects on PSII function. Such preparations show large decreases in steady state oxygen evolution rates, and S-state defects including stabilization of the S_2 state lifetimes, and slowing of the $S_2 \rightarrow S_3$ transition. Chloride is necessary for S-state advancement in both the $S_2 \rightarrow S_3$, and $S_3 \rightarrow S_4 \rightarrow S_0$ transitions (Wincencjusz, et al., 1997). Removal of the extrinsic proteins from PSII results in a requirement for high, non-physiological concentrations of both calcium and chloride to maintain some oxygen-evolving activity (Bricker, et al., 2011). In PSII membranes depleted of PsbO, and also in *Synechocystis* mutants lacking the gene encoding PsbO, two manganese atoms were lost at chloride concentrations less than 100 mM (Kuwabara et al., 1985; Burnap et al., 1994). In both the higher plant and cyanobacterial systems, removal of the PsbO protein resulted in increases in the S_2 and/or S_3 lifetimes (Miyao et al., 1987; Burnap et al., 1992; Liu et al., 2007) and also in a slowing of the $S_3 \rightarrow S_4 \rightarrow S_0$ transition (Ono & Inoue, 1985; Burnap et al., 1992; Liu et al., 2007). Removal of the PsbP and PsbQ extrinsic proteins in higher plant PSII also results in a large decrease in oxygen-evolving activity, which can be

partially restored by high concentrations of calcium and chloride (Popelkova & Yocum, 2007). The absence of these proteins also makes the Mn_4CaO_5 cluster vulnerable to the effects of exogenous reductants (Ghanotakis et al., 1984).

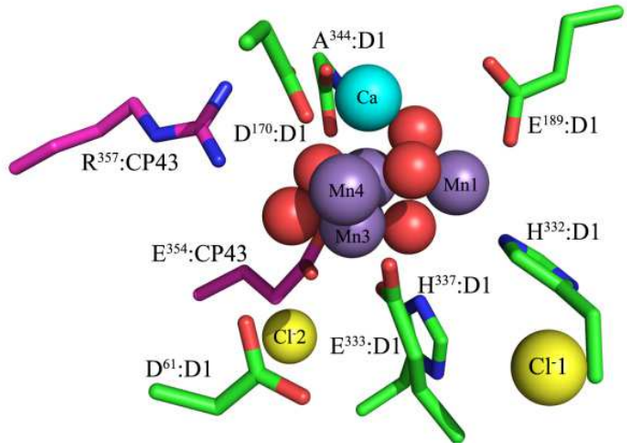

Fig. 1. Coordination Environment of the Mn_4CaO_5 Cluster.
The amino acid residues in the first and second coordination sphere are labeled. Please note that D342:D1 is obscured in this view by the metal cluster. The manganese ions are shown in purple and are labeled. Calcium is shown in cyan and the oxygens are shown in red. The proximal and distal chlorides are shown in yellow and labeled Cl^-1 and Cl^-2, respectively. This figure was generated in Pymol from the crystal structure of *Thermosynechococcus vulcanus* (PDB: 3ARC; Umena et al., 2011).

In cyanobacteria, deletion of the PsbU protein results in a mutant capable of growth in normal media, but which shows a reduced growth rate in media depleted of chloride (Shen et al., 1997). This mutant has reduced rates of oxygen evolution, a more stable S_2 state, and is more susceptible to damage to its PSII centers by both light and heat stress (Shen et al., 1997; Shen et al., 1998; Inoue-Kashino et al., 2005). Mutants constructed by deletion of the extrinsic cytochrome c_{550} protein, encoded by the *psb*V gene, do not grow well photoautotrophically, and exhibit no capacity for photoautotrophic growth in media depleted of either calcium or chloride (Shen et al., 1998; Katoh et al., 2001). The *psb*V deletion mutants also show decreased ability to evolve oxygen and reduced numbers of PSII centers in the thylakoids (Shen et al., 1995; Katoh et al., 2001). They also exhibit S-state cycling defects, including an increase in miss and double hit factors and a slowing of the $S_3 \rightarrow S_4 \rightarrow S_0$ transition (Shen et al., 1998).
These observations are all supportive of a role of the extrinsic proteins in maintaining the proper ionic environment around the Mn_4CaO_5 cluster. How chloride is actually bound and transported to the active site is currently unknown. Interestingly, the current crystal structure identified a third chloride ion bound near the C-terminal amino acid of PsbU, which is located between PsbU and cytochrome c_{550} (Umena et al., 2011; Kawakami et al., 2011). This chloride is ligated by water molecules and lies close to the exit of a proposed hydrogen-bonding network leading from the Mn_4CaO_5 cluster to the lumen that could possibly serve to transport anions, water or protons (Gabdulkhakov et al., 2009; Vassiliev et al., 2010; Kawakami et al., 2011).

4. Structure and function of CP43

The product of the *psb*C gene, the CP43 mature protein from *Synechocystis* 6803 consists of 460 amino acid residues and is well conserved. The nucleotide sequence of *psb*C has been determined from more than 50 species. The predicted plant apoproteins show approximately 95% homology with each other, and 85% and 77% homology with *Chlamydomonas* and cyanobacterial CP43, respectively. Early crystallographic studies confirmed that CP43 contains six transmembrane alpha helices (Zouni et al., 2001; Kamiya and Shen, 2003; Ferreira et al., 2004). The transmembrane helices of CP43 contain a number of conserved histidyl residues that function as chlorophyll-*a* ligands. Replacement of these histidyl residues with either tyrosyl or arginyl residues (Shen et al., 1993) results in mutants showing decreased PSII stability and defects in light-harvesting efficiency. Thirteen chlorophyll-*a* molecules associated with CP43 were assigned in the most current crystal structure (Umena et. al., 2011).

In addition to the six transmembrane alpha helices, CP43 contains five hydrophilic loops that connect the membrane-spanning domains. The positions of these loops are as follows (*Synechocystis* 6803 numbering): Loop A, Glu58-Phe98; Loop B, Gly123-Thr145; Loop C, Gly170-Asp219; Loop D, Lys242-Tyr258 and Loop E, Asn280-Arg410. Loop E, with 130 amino acids, is quite large and contains approximately 30% of the amino acids in this protein. Loops A, C and the large extrinsic Loop E are exposed to the lumenal side of the thylakoid membrane. The N- (Val1-Lys36) and C-termini (Arg448-Asp460), in addition to Loops B and D, face the stromal surface of the membrane (von Heijne and Gavel, 1988; Sayre and Wrobelboerner, 1994;). The CP47 protein has a similar structure and also possesses a large extrinsic loop.

All crystal structures of dimeric PSII show that CP43 is positioned on the D1 side of the D1-D2 heterodimer and CP47 on the D2 side. The two PSII monomers are related by a local-C2 rotation axis oriented perpendicular to the plane of the membrane. CP47 lies at the interface of the two monomers while CP43 is located at the periphery. This location is speculated to be necessary for the removal and replacement of damaged D1 during photoinhibition. In both CP43 and CP47, the six transmembrane helices are arranged as a "trimer of dimers". The large extrinsic loop of CP47 lies adjacent to the PsbO protein, consistent with a large body of biochemical evidence (Bricker & Frankel, 2002), and is also close to the extrinsic PsbU protein. The large extrinsic loop of CP43 is located adjacent to cytochrome c_{550} and PsbU, as well as the manganese cluster.

Early mutagenesis and biochemical studies clearly outlined a role for CP43 in oxygen evolution and the stable assembly of the PSII complex. CP43 is required for optimal oxygen-evolving activity from isolated PSII preparations (Bricker, 1990). *Chlamydomonas* strains incorporating mutations that affected either the synthesis or stability of CP43 were deficient in PSII activity (Rochaix et al., 1989). In these mutants, levels of the other PSII core proteins were severely reduced. *Synechocystis* mutants lacking the *psb*C gene as a result of deletion mutagenesis accumulated PSII core complexes (minus CP43) to only 10% of wild-type levels and could not grow photoautotrophically or evolve oxygen (Rogner et al., 1991; Carpenter et al., 1990). Interruption of the *psb*C gene by insertional mutagenesis also produced a mutant incapable of evolving oxygen, but which exhibited primary charge separation (Vermaas et al., 1988). A S*ynechocystis* mutant recovered by nitrosoguanidine mutagenesis was unable to evolve oxygen or support PSII electron transport from water to either dichlorobenzoquinone or methyl viologen (Dzelzkalns & Bogorad, 1988). Further characterization of this mutant

showed that it contained a short deletion within the *psb*C gene. Thylakoid membranes isolated from this mutant had decreased levels of the reaction center protein D2.

In studies specifically targeting the large extrinsic loop E of CP43, eight short deletions were produced in *Synechocystis* CP43 (Kuhn & Vermaas, 1993). Significantly, all resulting mutants showed complete loss of photoautotrophic growth and the ability to evolve oxygen. These mutants also contained decreased levels of the PSII reaction center proteins D1, D2 and CP47. This work clearly established a role for the large extrinsic loop in PSII function.

Site-directed mutagenesis of the large extrinsic loop of CP43 in *Synechocystis* has revealed a number of amino acids required for normal PSII function. In general, these mutants segregate into two groups. One group contains mutations at residues that appear to be involved in manganese ligation and catalysis. These sites are Glu354 and Arg357. Glu354 and Arg357 lie, respectively, within the first and second coordination spheres of the Mn_4CaO_5 cluster. Glu354, as stated above, provides bidentate ligation of Mn3, and also binds one chloride ion. The effects of mutation of this residue have been examined in three independently constructed mutants in which the glutamate was replaced with glutamine (Rosenburg et al., 1999; Strickler et al., 2008; Shimada et al., 2009; Service et al., 2011). The E354Q mutant grows slowly and exhibits only 20% of control rates of oxygen-evolving activity. The PSII centers of this mutant can advance to the S_2 and S_3 states, but do not advance past S_3 (Shimada et al., 2009; Service et al, 2011). Glu354 appears to ligate manganese bound to a substrate water molecule (Shimada et al., 2009; Service et al, 2011) that undergoes rapid exchange in the S_3 state (Service et al., 2011). Arg357 lies in the second coordination sphere of the Mn_4CaO_5 cluster. In the crystal structure, one guanidinium nitrogen of this residue is hydrogen-bonded to two of the μ-oxo bridges (O2 and O4) and the other is hydrogen-bonded to two residues of the D1 protein, Asp170, which ligates Mn4 and the calcium ion, and Ala344, which ligates Mn2. Mutation of this arginine to serine abolished oxygen-evolving activity and photoautotrophic growth (Knoepfle et al., 1999; Ananyev et al., 2005). A more conservative replacement of the arginine with lysine (Hwang et al., 2007), also produced a mutant that failed to grow photoautotrophically but retained a low rate of oxygen-evolving activity. S-state cycling defects were observed in this mutant. Specifically, the strain exhibited a high miss factor and a decreased yield of the S_2 state. Using isotopic labeling coupled with FTIR spectroscopy, structural coupling between an arginine and the Mn_4CaO_5 cluster was observed (Shimada, et al., 2011). The arginine was presumed to be Arg357 of CP43, since this is the only arginine residue in close proximity to the Mn_4CaO_5 cluster. The data are consistent with a role for Arg357 in the structural stabilization of the cluster and/or possibly in abstracting protons during water oxidation, as has been proposed previously (McEvoy & Brudvig, 2006). These experimental data are consistent with the crystallographic data and with a direct role of both Glu354 and Arg357 of CP43 in the water splitting mechanism.

Of particular interest is a second group of CP43 mutants showing defects associated with the chloride requirement of PSII. These are mutations at Arg320 and Asp321. We have extensively characterized a *Synechocystis* mutant in which Arg320 was replaced by serine (Knoepfle et al., 1999; Young, et al., 2002). When grown in complete BG-11 media (480 μM chloride), the R320S mutant strain exhibited photoautotrophic growth rates comparable to the control strain and assembled approximately 70% of the PSII centers found in the control strain (Knoepfle et al., 1999). These centers are capable of evolving oxygen to 60-70% of

control rates at saturating light intensities. However, they show an enhanced susceptibility to photoinactivation. Additionally, the fluorescence rise time for this mutant was increased by a factor of two over the control. Thus, the PSII centers in this mutant do not function normally, even under normal growth conditions. Significantly, when the R320S mutant was grown in media depleted of chloride (30 μM chloride), it exhibited a severely reduced photoautotrophic growth rate. The effect of chloride depletion on the growth rate of the mutant was reversed by the addition of 480 μM bromide to the chloride-depleted BG-11 media. It is well known that bromide will functionally replace chloride at the oxygen-evolving site in cyanobacteria grown on bromide-containing media (Yachandra et al., 1993). Additionally, it is well known that bromide can replace chloride in supporting oxygen evolution in isolated thylakoids (Kelly & Izawa, 1978) and PSII membranes (Sandusky & Yocum, 1983). Oxygen evolution rates for the mutant were further depressed to about 22% of the rate observed in control cells under chloride-limiting conditions. Addition of bromide restored these rates to those observed under chloride-sufficient conditions. The mutant exhibited a significantly lower relative quantum yield for oxygen evolution than did the control strain and this was exacerbated under chloride-limiting conditions. Fluorescence yield measurements indicated that both the mutant and control strains assembled fewer PSII reaction centers under chloride-limiting conditions. The reaction centers assembled by the mutant exhibited an enhanced sensitivity to photoinactivation under chloride-limiting conditions, with a $t_{1/2}$ of photoinactivation of 2.6 min under chloride-limiting conditions compared to a $t_{1/2}$ of 4.7 min under normal growth conditions. The mutant also exhibited an enhanced stability of its S_2 state and an increased number of centers in the S_1 state following dark incubation. These results indicate that the mutant R320S exhibited a defect in its ability to utilize chloride in support of efficient oxygen evolution in PSII. This was the first mutant of this type described in the CP43 protein**.** In terms of this chloride effect, R320S has a similar phenotype to the R448G, K321G, and F363R mutants constructed in the CP47 large extrinsic loop (Putnam-Evans & Bricker, 1994, 1997; Clarke & Eaton-Rye, 1999). These results were significant because the R320S mutation represented the first site in the CP43 protein that alters the chloride requirement of PSII and inferred that the large extrinsic loop of CP43 is involved in chloride binding/sequestration at the PSII active site.

The phenotype of R320S closely resembles that of mutants in which the extrinsic cytochrome c_{550} protein has been deleted. Cytochrome c_{550} appears to regulate the efficiency of the $S_1 \rightarrow S_2$ and/or the $S_2 \rightarrow S_3$ state transitions. The *psb*V deletion strains exhibit a stabilization of the S_2 state and cannot grow photoautotrophically under chloride- or calcium-limiting conditions (Shen et al., 1998). Cytochrome c_{550} functions in a manner similar to that of the PsbP protein in higher plant PSII. We recently have shown that R320S also does not grow under conditions of calcium depletion (Putnam-Evans, unpublished). In order to assess whether or not cytochrome c_{550} is associated with PSII in the mutant, a histidine-tagged version of the R320S mutant was produced to facilitate the isolation of PSII particles. These particles were analyzed for the presence of cytochrome c_{550} (Bricker et al., 2002). Reduced minus oxidized difference spectroscopy and chemiluminescence staining on western blots indicated that cytochrome c_{550} was absent in these PSII particles. Whole cell extracts from the R320S mutant, however, contained a similar amount of cytochrome c_{550} to that observed in the control strain. These results indicate that the mutation R320S in CP43 prevents the strong association of cytochrome c_{550} with the PSII core complex. Thus, the Arg320 residue may be involved in the formation of the binding domain for the cytochrome. This is the first

residue identified in any PSII protein that potentially provides a binding site for cytochrome c_{550}. We have also begun preliminary investigation of mutants produced at the residue adjacent to Arg320, Asp321. Replacement of this aspartate by asparagine produced a mutant with a phenotype very similar to that of the R320S mutant (Putnam-Evans, unpublished). That is, this mutant exhibits almost normal PSII function when grown in complete BG-11 media, but fails to grow photoautotrophically under chloride-limiting conditions and exhibits a marked decrease in oxygen evolution rates under chloride depletion.

Examination of the newest crystal structure reveals that Arg320 lies at the interface between cytochrome c_{550} and PsbU, within 2.9 angstroms of Asn49 of cytochrome c_{550}, close enough to form a hydrogen bond. Another potential hydrogen bonding partner in *Synechocystis* is Asn51. However, in *Thermosynechococcus*, the organism from which the x-ray structure is derived, this residue is a serine residue. Nevertheless, it is located only 3.6 angstroms from Arg320. Asp321 lies within 2.7 angstroms of Asn99. Additionally, Arg320 and Asp321 of CP43 lie within 2.8 angstroms of each other. Thus, these sites are candidates for potential ligands to cytochrome c_{550} and PsbU. It is tempting to speculate that Arg320 of CP43 is a central player in these interactions, perhaps via a hydrogen bonding network involving several of these and perhaps other residues. Here we report the construction and preliminary characterization of two additional mutations at site 320, R320D and R320K, towards the goal of better understanding the role of this amino acid in these potential protein-protein interactions in PSII.

5. Experimental methods

5.1 Growth conditions and growth measurements

Control and mutant *Synechocystis* 6803 were grown in liquid BG-11 media (Williams, 1988) at 30°C and a light intensity of 25 μmol photons*m^{-2}*s^{-1}, with shaking at 200 rpm on a rotary shaker. Glucose was added, when appropriate, to a final concentration of 5 mM (photomixotrophic growth). For fluorescence measurements, the BG-11 media was supplemented with 5 mM glucose and 10 μM N'-(3,4-dichlorophenyl)-N,N-dimethylurea (DCMU). Antibiotics were added to the medium to a final concentration of 10 μg/ml. For growth on solid media, BG-11 media was supplemented with 1.5 % agar, 0.3 % sodium thiosulfate, and 10 mM N-tris-(hydroxymethyl)methyl-2-aminoethanesulfonic acid/potassium hydroxide (TES/KOH), pH 8.2, and 10 μM DCMU.

For growth under chloride-limiting conditions, chloride was excluded from the media by the addition of calcium nitrate, cobalt nitrate, and manganese sulfate in place of their respective chloride salts. To prevent the leaching of chloride from glass, polycarbonate flasks and carboys were used for growing these cultures. BG-11 prepared in this manner contains approximately 30 μM chloride as compared to normal media, which has a chloride concentration of 480 μM (Young et al., 2002). For growth assessment, cells were grown as above and the OD_{730} was determined at the same time each day for 9 days.

5.2 PCR and DNA sequencing

Genomic DNA was isolated as follows: A small ball of cells was scraped from a culture grown on solid media. The cells were washed with liquid BG-11 media and pelleted by centrifugation at 3326 x *g* for 1 minute. The pelleted cells were resuspended in 400 μl 5 mM Tris-HCl, pH 8.0, 50 mM NaCl, 5 mM EDTA. Next, 100 μl of lysozyme (50 mg/ml in dH_2O)

was added and the mixture was incubated at 37°C for 15 minutes. Then, 20 µl of 500 mM EDTA, 50 µl of proteinase K (10 mg/ml in 50% glycerol), and 55 µl of 10% sarkosyl were added. The mixture was then incubated at 55°C for 15 minutes. After 5 minutes at room temperature, 600 µl of TE (5 mM Tris-HCl, pH 8.0, 5 mM EDTA) saturated phenol was added and the mixture incubated at room temperature for 10 additional minutes with gentle inversion. The mixture was then centrifuged at 18000 x *g* for 3 minutes and the aqueous phase was transferred to a new tube. Next, 100 µl of 5 M NaCl, 100 µl of 10% CTAB, and 600 µl of chloroform were added to the sample. The tubes were then shaken on a rotary shaker for 15 minutes, centrifuged at 8300 x *g* for 3 minutes, and the aqueous phase was transferred to a new tube. Next, an equal volume of cold 100% isopropanol was added to the sample, and the tubes were gently inverted. The mixture was allowed to incubate at room temperature for 20 minutes to precipitate the DNA before centrifuging the sample at 8200 x *g* for 10 minutes at 4°C to pellet the DNA. After centrifugation, the supernatant was removed and discarded, and 1 ml of cold 70% ethanol was added to the tube to wash the DNA pellet. The tubes were then centrifuged again for 10 minutes at 4°C. Following this, the supernatant was quickly removed and the DNA pellet was allowed to air dry. Then, 100 µl of TE buffer was added to the tube and the DNA was allowed to resuspend at room temperature overnight. Afterward, the DNA was stored at 4°C.

The *psbC* gene was amplified by PCR. A typical reaction consisted of 79.7 µl of sterile dH_2O, 10 µl of 10X PCR buffer (Invitrogen, Inc.), 4 µl of 50 mM $MgCl_2$, 0.8 µl of 10 mM dNTPs, 2 µl of forward primer (2 pmol/µl) (Invitrogen, Inc.), 2 µl of reverse primer (2 pmol/µl) (Invitrogen, Inc.), 30-60 ng of genomic DNA, and 0.5 µl of Taq DNA polymerase (2.5 units, recombinant). The thermal cycling routine consisted of the following steps: Step 1 – 1 cycle of 94°C for 3 minutes, 60°C for 45 seconds, and 72°C for 2 minutes, Step 2 – 25 cycles of 94°C for 1 minute, 60°C for 45 seconds, and 72°C for 2 minutes, Step 3 – 5 cycles of 94°C for 1 minute, 60°C for 45 seconds, and 72°C for 2 minutes with a 5 second extension added to the elongation step each cycle, and Step 4 – 72°C for 7 minutes.

Samples were cleaned using a QIAquick PCR Purification Kit (Qiagen, Inc.) and resuspended in 40 µl of sterile dH_2O. Following the cleanup, the samples were subjected to sequencing reactions in a PTC-100™ Programmable Thermal Cycler (MJ Research, Inc.). The components of these sequencing reactions were 5 µl of sterile dH_2O, 2 µl of Big Dye (Applied Biosystems, Inc.), 3 µl of Big Dye reaction buffer, 2 µl of primer (2 pmol/µl), and 30-60 ng of purified PCR product DNA. The cycling routine was as follows: 26 cycles of 94°C for 1 minute, 55°C for 1 minute, and 72°C for 2 minutes, followed by a final elongation at 72°C for 10 minutes.

After the completion of the sequencing reactions, the DNA was alcohol precipitated with ethanol and was resuspended in a 5:1 formamide:50 mM EDTA/50 mg/ml Blue Dextran mixture. Then, samples were loaded in an ABI Prism 377 DNA Sequencer (Applied Biosystems, Inc.) and the sequencer was run for 7 hours. Sequences were analyzed using the Auto Assembler DNA sequence analysis software (Applied Biosystems v.1.4.0).

5.3 Oxygen evolution assays and photoinactivation assays

Oxygen evolution activity was measured by O_2 polarography with a Hansatech oxygen electrode (Knoepfle et al., 1998). Assays were performed at 25°C on whole cells in complete or chloride-depleted BG-11 media with 1 mM 2,6-dichlorobenzoquinone (DCBQ) added as

an artificial electron acceptor. Cells were allowed to grow for 5 days under the appropriate growth conditions, as above, and were harvested on the fifth day by centrifuging at 12000 x *g* for 5 minutes at 4°C. The cells were then resuspended in 1-2 ml of complete BG-11 media. Next, the chlorophyll concentration of each sample was determined by taking absorbance readings at 678 nm and 710 nm and calculating the concentration of chlorophyll (in μg/ml) by the equation: $(OD_{678}-OD_{710}) * 14.96 *$ dilution factor (modified from Williams, 1988). The light intensity used during these assays was 2500 μmol photons*m^{-2}*s^{-1} of white light, verified with a spectroradiometer equipped with a quantum probe (Li-Cor, Inc.).
For photoinactivation experiments, cells were incubated at 25°C in BG-11 media, at a chlorophyll concentration of 10 μg/ml, and exposed to a light intensity of 5000 μmol photons*m^{-2}*s^{-1}. Cells were removed from exposure to the photoinactivating light in increments of 2 minutes and assayed for oxygen-evolving activity, as above. The $t_{0.5}$ for photoinactivation was calculated by fitting the data to a single exponential decay.

5.4 Fluorescence measurements

Fluorescence yield measurements were performed on a Waltz PAM 101 fluorometer as described previously (Nixon & Diner; 1992, Chu et al., 1994). Samples were incubated in the dark for 5 minutes in the presence of 1 mM potassium ferricyanide and 330 μM DCBQ. Next, DCMU was added to a final concentration of 40 μM followed one minute later by the addition of hydroxylamine hydrochloride, pH 6.5, to a concentration of 20 mM. After 20 s, the weak monitoring flashes were turned on, followed 1 s later by continuous actinic illumination (1000 μmol photons*m^{-2}*s^{-1}). The variable fluorescence was measured and a second set of assays was performed, this time omitting the hydroxylamine, in order to measure the variable fluorescence with water as the electron donor. For both assays, F_{max} was measured 5 s after the onset of actinic illumination.

5.5 Introduction of poly-histidine tags and purification of photosystem II

A recombinant pTZ18 plasmid was created previously that contained the *psbB* gene encoding CP47 with six histidyl codons at the 3′ end of the gene (Young et al., 2002). An antibiotic resistance gene encoding resistance to spectinomycin was cloned into the 3′ non-coding portion of the *psb*B gene downstream of the His-tag. This plasmid was transformed into *Synechocystis* as previously described (Williams, 1988). Briefly, 5 x 10^8 cells in 100 μl of BG-11 media were added to a sterile 15 ml centrifuge tube. To these cells, 2.5 μg of plasmid DNA was added. The tubes were incubated for 4-6 hours at room temperature and exposure to a light intensity of 25 μmol photons*m^{-2}*s^{-1}. After incubation, the entire volume of cells was plated onto solid BG-11/glucose/DCMU to which no antibiotic had been added. After 48 hours, the plates were underlaid with antibiotic solution (196 μl of BG-11 media + 8 μl spectinomycin (50 mg/ml stock)). Transformants were allowed to sort out by serial streaking on BG-11 plates containing glucose, DCMU, and spectinomycin. The insertion of the histidyl codons was confirmed by DNA sequencing, as above.
Cells were grown in either complete BG-11 media or in BG-11 media deficient in chloride. Cultures were supplemented with 5 mM glucose and 5 μg/ml spectinomycin. The cells were grown at 25°C, with aeration, at a light intensity of 25 μmol photons*m^{-2}*s^{-1}, for 7-9 days. Cells from 15 l cultures were centrifuged 10000 x *g* for 10 minutes at 4°C. The cells were resuspended in an adequate amount of Buffer A (50 mM 2-(N-morpholino)ethanesulfonic acid (MES)-NaOH, pH 6.0, 10 mM $MgCl_2$, 5 mM $CaCl_2$, 25% glycerol) (~10 ml per pellet),

combined into a single container, and centrifuged again at 10000 x *g* for 10 min at 4°C. Excess Buffer A was decanted and the pellet was frozen at –70 °C.

To purify the His-tagged PSII, the procedure of Bricker et al. (1998) was used. Frozen cells were thawed and resuspended in 5 ml of Buffer A. The cells were then assayed for chlorophyll concentration and brought to 1 mg/ml of chlorophyll. Then, the cell suspension was brought to 1.0 mM phenylmethylsulfonyl fluoride (PMSF), 1.0 mM benzamidine, 1 mM ε-amino caproic acid, and 50 μg/ml DNAase. The sample was added to an ice water cooled bead beater apparatus (Bio-Spec Products, Inc.) and glass beads (1.0 mm) were added at a 1:1 ratio to the cell suspension. The cells were then broken at 4°C over 12-14 break cycles, each consisting of 15 seconds of homogenization followed by 4 minutes of cooling. The cell homogenate and glass beads were then transferred to a beaker and the glass beads allowed to settle. The cell homogenate was decanted and the beads were washed several times with Buffer A to recover additional homogenate. The cell homogenate was brought to 1% n-dodecyl-β-D-maltoside by the addition of a 10% n-dodecyl-β-D-maltoside stock solution (freshly prepared) and was immediately centrifuged at 36000 x *g* for 10 minutes to remove unbroken cells and residual glass beads. The solubilized cell homogenate was then loaded onto a 25 ml cobalt metal affinity column (Clontech, Inc.) which had been pre-equilibrated with Buffer A + 0.04% n-dodecyl-β-D-maltoside at 4°C. The column was washed with several bed volumes of Buffer A + 0.04% n-dodecyl-β-D-maltoside and the bound His-tagged PSII particles were eluted with Buffer A + 0.04% n-dodecyl-β-D-maltoside + 50 mM L-histidine. The eluted fractions were then pooled and the PSII complex was precipitated by addition of an equal volume of 25% PEG-8000 in 50 mM MES-NaOH, pH 6.0, and incubation at 4°C for 30 minutes. The precipitated PSII particles were harvested by centrifugation at 36000 x *g* for 30 minutes. The precipitated PSII particles were resuspended in 1.0 ml of Buffer A + 0.04% n-dodecyl-β-D-maltoside and stored immediately at –70 °C.

5.6 Spectrophotometric assays

For the determination of absorbance spectra, the procedure of Bricker and coworkers (2002) was employed. First, purified PSII particles were assayed for chlorophyll concentration by methanol extraction, and samples were diluted to 20 μg/ml chlorophyll in a solution of 50 mM MES-NaOH, pH 6.5, 10 mM $MgCl_2$, 5 mM $CaCl_2$, 50 mM NaCl, 0.04% β-D-dodecyl maltoside, and 25% glycerol. After performing a baseline correction on a Cary 100 dual-beam spectrophotometer (Varian, Inc.), the samples were either oxidized with a few crystals of potassium ferricyanide, for the reference cuvette, or reduced with a few crystals of sodium dithionite, for the sample cuvette. After a 10-minute dark incubation, reduced minus oxidized difference spectra were collected by scanning the samples from 540-580 nm for the cytochrome-specific spectra, and from 400-800 nm for the overall absorbance spectra.

6. Results

6.1 Verification of genomic DNA sequence

The charge-switching mutants constructed for this study were created by site-directed mutagenesis of Arg320 of CP43 to either lysine or aspartate. DNA sequencing of the portion of the *psbC* gene surrounding the mutation site was used to verify each point mutation. Additionally, because the mutant sequence was engineered within a plasmid insert

containing the AccI/AccI fragment of *psbC*, the DNA sequence included between these restriction sites in the genomic DNA was also sequenced. This segment consists of 1221 base pairs, along with an inserted kanamycin resistance cartridge. DNA sequencing confirmed the presence of the desired point mutations, as well as the integrity of the sequence within the AccI/AccI fragment.

Additional mutants were created for the insertion of a poly-histidine tag on the CP47 protein of control and mutant strains. This was done by inserting a series of six consecutive histidine-encoding codons, along with a spectinomycin resistance cartridge, into *psb*B. The poly-histidine encoding sequence was verified by DNA sequencing for each strain.

6.2 Growth measurements

The mutant and control strains were grown in the absence of glucose to determine the effect of each mutation on the photoautotrophic growth characteristics of the organism. Each strain was grown in complete BG-11 media, in BG-11 media deficient in chloride, or in chloride-deficient BG-11 media supplemented with 480 μM sodium bromide, in order to determine any effect chloride had on the growth of the strains. In complete media, both R320K and R320D grew at rates comparable to the control strain (Fig. 2A). In chloride-deficient media, the control strain exhibited a normal growth rate. (Fig. 2B). The mutant strains, however, were affected under these conditions, with R320K growing at a lower rate than it did in complete media and R320D showing virtually no photoautotrophic growth. When the strains were grown in chloride-deficient media supplemented with bromide (Fig. 2C), growth rates for each mutant strain were restored to near those observed for the strains grown in complete media. It is well known that bromide can substitute for chloride at the PSII active site (Sandusky & Yocum, 1983; Yachandra et al., 1993).

6.3 Oxygen evolution

Oxygen evolution rates were measured for control and mutant strains grown either photoautotrophically or in the presence of glucose. When grown photoautrophically (Fig. 3), the control strain evolved oxygen at similar rates regardless of the media conditions. In complete media, the R320K strain evolved oxygen at a rate about 80% that of the control. When chloride was lacking in the growth media, this rate fell to 35% of the control. The R320D strain was the least successful of these strains for evolving oxygen. When grown photoautotrophically in complete media, the rate of oxygen evolution for this strain was depressed to 60% of the control. The effect on oxygen evolution was greatly exacerbated when the strain was grown under chloride-limiting conditions, where the observed rate of oxygen evolution was only 5% of the control rate. For both mutants, the addition of bromide restored this rate to levels near those observed for cells grown in complete media. These same results were observed when the strains were grown photomixotrophically (not shown).

6.4 Variable fluorescence yields

Variable fluorescence yield assays are used to make qualitative estimates of the number of PSII centers present in the thylakoid membranes of a particular strain, and also allow for a determination of the functionality of these centers. The results of these experiments for cells grown in complete media are shown in Table 1. Both mutant strains assemble relatively

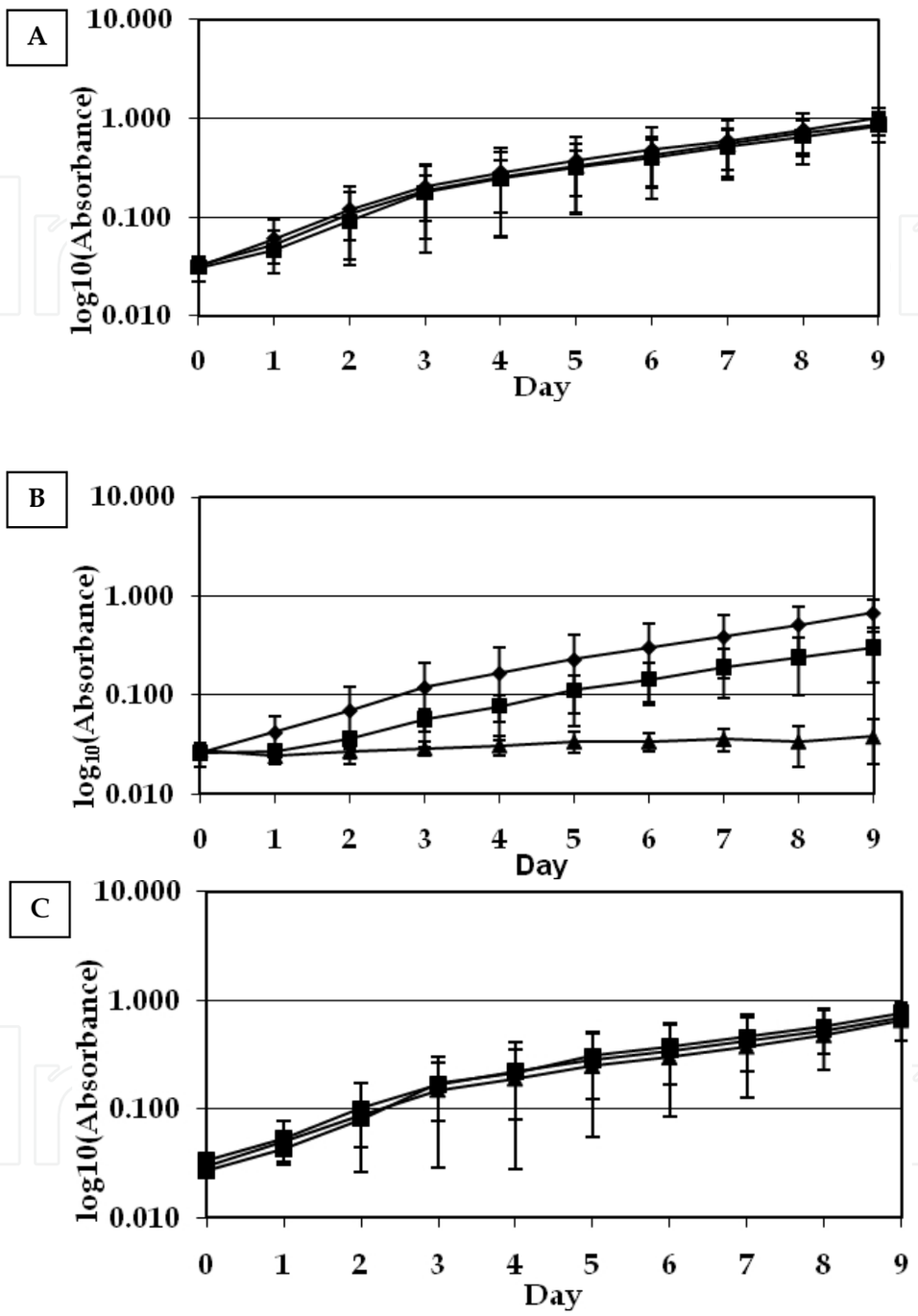

Fig. 2. Photoautrophic Growth of Mutant and Control Strains.
Growth curves showing control (diamonds) and mutant strains (R320K squares; R320D triangles) grown in either **A.** complete media, **B.** chloride-deficient media, or **C.** chloride-deficient media supplemented with bromide. These results are the average of at least 3 independent experiments. The error bars represent plus and minus one standard deviation.

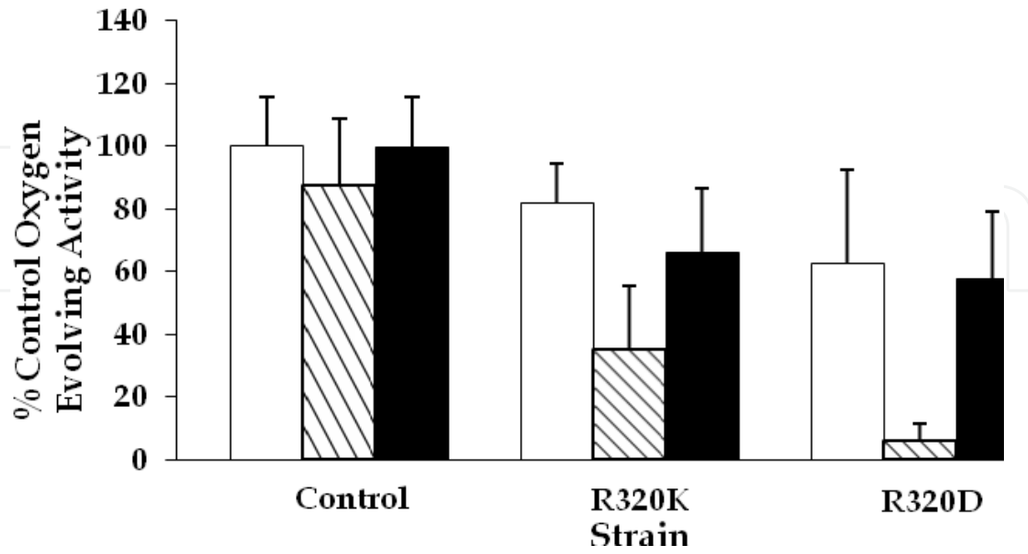

Fig. 3. Oxygen Evolution Rates of Control and Mutant Strains Grown Photoautotrophically. The control rate in complete media was 391 µmol O_2*(mg chlorophyll)-1 *hr-1. Rates are expressed as the percentage of the control rate in cells grown in complete media. White bars, oxygen evolution rates from cells grown in complete media; Striped bars, oxygen evolution rates from cells grown in chloride deficient media; Black bars, oxygen evolution rates from cells grown in chloride depleted media with 480µM bromide added. The results are the average of at least three independent experiments. The error bars represent plus and minus one standard deviation.

large numbers of PS II centers that can transfer electrons from hydroxylamine to Q_A. R320K and R320D assembled 80% and 83%, respectively, of the PS II centers assembled in the control strain. If water is used as an electron donor, the variable fluorescence yield is a measure of the amount of PSII centers that can oxidize water. The data from the water experiment indicate that the mutant centers remain mostly functional under normal growth conditions, with the fluorescence yields for both mutants being approximately 80% that of the control strain. Data is also included for the psbC deletion strain, which lacks any functional PSII centers. Data for the R320S mutant (Young et al., 2002) is also included and shows that this mutant, like R320D and R320K, contains substantial numbers of PSII centers that are efficient in water oxidation.

6.5 Photoinactivation

Photoinactivation assays are used to determine the relative stability of the PSII complex of a strain. As summarized in Table 2, when grown photoautotrophically, regardless of the media, the control strain had a $t_{0.5}$ for photoinactivation of approximately 5.6 min. In complete media, R320K exhibited a $t_{0.5}$ close to the control of 5.3 min and R320D a $t_{0.5}$ slightly lower than the control of 3.6 min. When grown in media deficient in chloride, however, the

mutant strains exhibited large increases in photoinactivation demonstrated by $t_{0.5}$ values of 2.9 and 0.9 min, respectively, for R320K and R320D. These data indicate that the PSII complexes of the mutants are less stable, and are much more susceptible to the effects of photoinactivating light intensities. It should be noted that the $t_{0.5}$ values for the R320K closely mirror those of the R320S mutant (Young et al., 2002).

Strain	Hydroxylamine	Water
Control	0.46 ± 0.069	0.45 ± 0.056
*psb*C Deletion	0.02 ± 0.000	-0.02 ± 0.029
R320K	0.37 ± 0.034	0.35 ± 0.022
R320D	0.38 ± 0.029	0.33 ± 0.020
R320S*	0.41 ± 0.030	0.46 ± 0.050

Table 1. Variable Fluorescence Yields.
Results of variable fluorescence yield assays performed on control, *psbC* deletion, R320K, and R320D, and R320S* strains.
(* Results for the R320S (R320S) strain obtained from Young et al., 2002. The control values for these experiments were hydroxylamine = 0.58 and water = 0.67.)

Strain	Complete Media	Chloride-Deficient Media
Control	5.4 min.	5.7 min.
R320K	5.3 min.	2.9 min.
R320D	3.6 min.	0.9 min.
R320S*	4.7 min.	2.6 min.

Table 2. $t_{0.5}$ Values for Photoinactivation.
$t_{0.5}$ values for photoinactivation for each strain after growth in either complete or chloride-deficient media and exposure to photoinactivating light (5000 μmol photons*m^{-2}*s^{-1}). The results are the average of at least two independent experiments.
(* Results from Young et al., 2002)

6.6 Visible absorption spectra

Absorbance spectra in the range of 400-800 nm were obtained for PSII particles purified from His-tagged control and mutant strains grown photomixotrophically in complete media. As can be seen in Fig. 4, there were no appreciable differences in these spectra, regardless of the strain, which indicates that no major disruption of the pigment-containing portion of PSII occurred within the mutant strains. The major peaks located at 410, 430, and 680 nm represent absorption by chlorophyll-a molecules, with the major peak at 680 nm representing the reaction center chlorophyll of PSII, P680. The minor peaks arise from accessory pigment molecules associated with the photosystem. These spectra are similar to spectra obtained from PSII preparations of non-His-tagged control strains (Noren et al., 1991; Tang & Diner, 1994) and to spectra obtained from other His-tagged PSII preparations (Bricker et al., 1998).

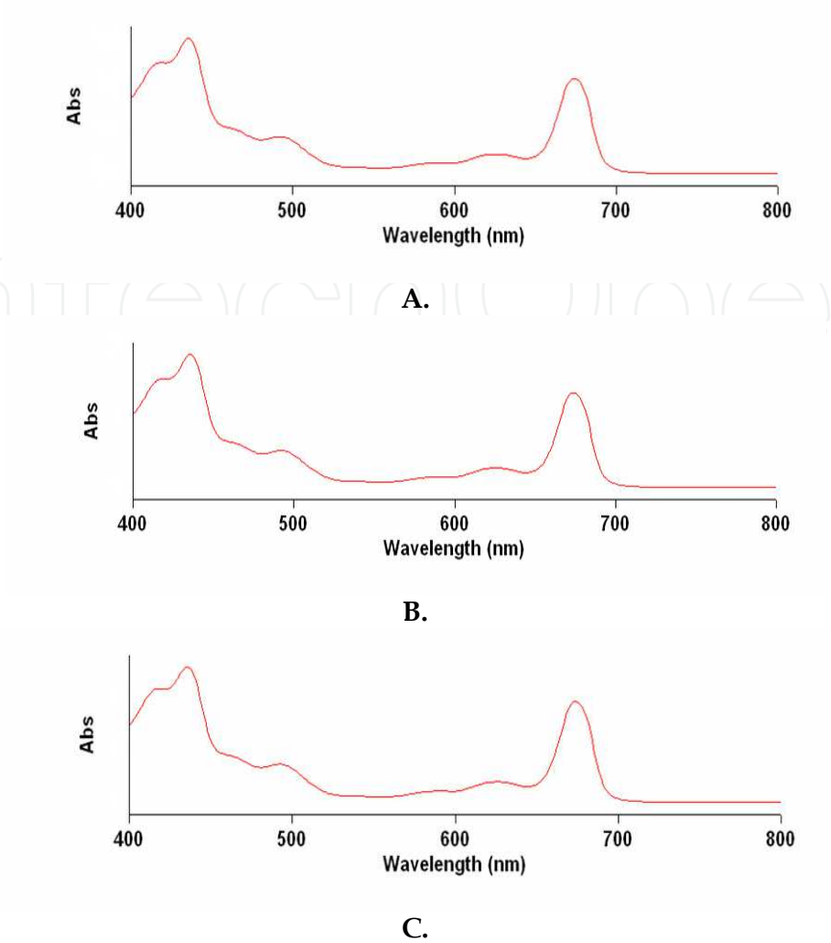

Fig. 4. Visible Absorption Spectra
Visible absorbance spectra for **A**. control, **B.** R320K, and **C.** R320D PSII histidine-tagged particles purified from cells grown photomixotrophically in complete BG-11 media.

6.7 Reduced-minus oxidized difference spectra

Reduced minus oxidized difference spectra were collected in the wavelength range of 540-580 nm for PSII particles isolated from the His-tagged control and mutant strains grown photomixotrophically in complete media (Fig. 5) Plots of the data reveal a non-symmetrical absorbance curve for the control strain. This non-symmetrical curve is also present in control PSII particles derived from cells grown under chloride depletion (not shown). This curve reveals a maximum absorbance at 559 nm that tapers off into a wide shoulder toward 550 nm, while toward 570 nm, there is no indication of a shoulder. The signal at 559 nm indicates the presence of cytochrome b_{559}, while the broadened shoulder arises due to the absorbance properties of cytochrome c_{550} (Bricker et al., 2002). The plots of data derived from the mutant strains, like the control, exhibit an absorbance maximum at 559 nm. However, unlike the control strain, the plots for the mutant strains are symmetrical, giving no indication of a broad shoulder on either side of the peak, regardless of the media, suggesting the absence of cytochrome c_{550} within these preparations. The same symmetrical peaks are observed for both mutants grown under chloride-limited conditions (not shown).

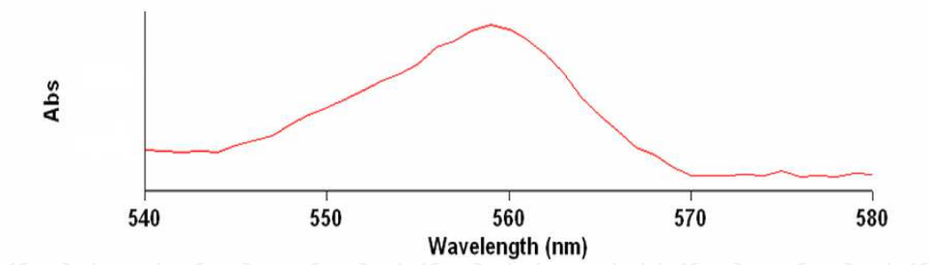

A.

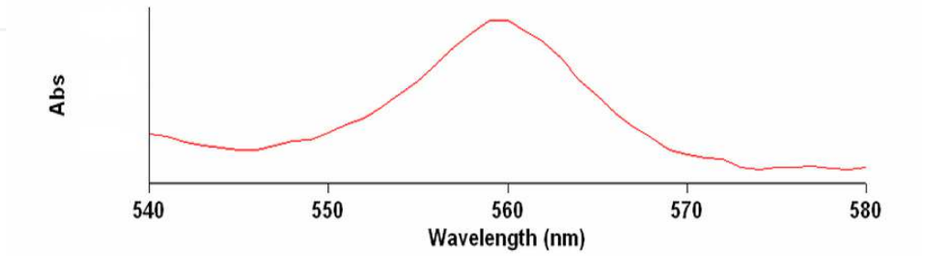

B.

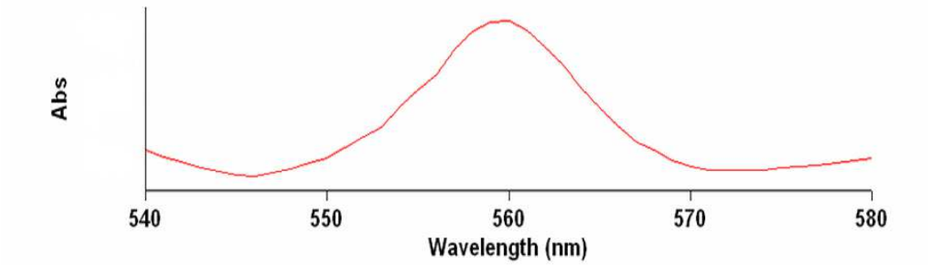

C.

Fig. 5. Reduced Minus Oxidized Difference Spectra

Reduced minus oxidized absorbance difference spectra for **A.** control, **B.** R320K, and **C.** R320D His-tagged PSII particles purified from cells grown photomixotrophically in complete media. Samples were diluted to 20 μg/ml chlorophyll in 50 mM MES-NaOH, pH 6.5, 10 mM $MgCl_2$, 5 mM $CaCl_2$, 50 mM NaCl, 0.04 % β-D-dodecyl maltoside, and 25 % glycerol. After performing a baseline correction on a Varian Cary 100 dual-beam spectrophotometer, the samples were either oxidized with a few crystals of potassium ferricyanide, for the reference cuvette, or reduced with a few crystals of sodium dithionite, for the sample cuvette. After a 10-minute dark incubation, reduced minus oxidized difference spectra were collected by scanning the samples from 580-540 nm. The peak absorbance at 560 nm measured approximately 0.10 absorbance units.

7. Discussion

The purpose of the present study was to elucidate further the interaction of CP43 with the extrinsic cytochrome c_{550} protein of PSII by studying the effect of additional alterations of the arginine residue at position 320 of the CP43 large extrinsic loop. Two additional mutations, R320K and R320D, were introduced into the large extrinsic loop and the effects of

each on PSII activity were characterized. First, the growth characteristics of the mutant strains were assessed. Under photoautotrophic growth conditions (Fig. 2A), when chloride levels in the media were not limiting, the control and mutant strains grew at the same rate. This indicates that under these growth conditions, there appear to be no discernible anomalies associated with PSII. When grown in chloride-deficient media, however, major differences arose. Under these conditions, the control strain grew at rates comparable to those in complete media, but R320D exhibited very little capacity for photoautotrophic growth (Fig. 2B). The R320K strain exhibited intermediate growth between that of the control and R320D. When grown in chloride-deficient media that had been supplemented with bromide, all strains grew at very similar rates, with the rates of the mutant strains being restored to those observed in complete media (Fig. 2C). As stated previously, bromide is well known to substitute for chloride at the active site of PSII, and these data clearly indicate that the effect on growth arises as a consequence of a defect associated with the chloride requirement of PSII.

Oxygen evolution rates were obtained for the control and mutant strains (Fig. 3). When grown photoautotrophically, the control strain evolves oxygen at similar rates, regardless of the media in which the cells are grown. The R320K strain exhibits a modest reduction in oxygen evolution rate when grown in complete media, which is greatly magnified when chloride is limiting in the media. Under these conditions, the R320K strain appears to evolve oxygen at less than 40% of the control strain. This rate is restored when bromide is included in the chloride-deficient media. The R320D strain reveals the most dramatic phenotype. When grown in complete media or in chloride-deficient media supplemented with bromide, this strain evolves oxygen at a rate of approximately 60% of the control strain. When chloride is limiting, however, this rate drops to only about 5% of that of the control strain. Taken together, these results indicate that there is a defect in both mutant strains in their ability to evolve oxygen, regardless of the media in which they are grown. This defect is exacerbated by a deficiency of chloride in the media, which again points to a physical and/or mechanistic defect at the PSII active site involving some interaction with chloride.

The data from growth experiments and oxygen evolution assays indicated that both mutant strains, which are relatively functional under normal growth conditions, must assemble a fairly normal content of PSII centers. Confirmation of this was obtained from variable fluorescence yield assays. These assays allow for a qualitative estimate of the number of PSII centers present when using hydroxylamine as an artificial electron donor to measure the reduction of Q_A (Nixon & Diner, 1992). The results presented in Table 1 show that the mutant strains assemble a near normal complement of PSII centers within their thylakoid membranes compared to the control strain. Thus, the mutations do not prevent the assembly and incorporation of PSII centers into the thylakoids of these strains.

When water is used as the electron donor, the variable fluorescence yield assay provides information on the functionality of the PSII centers present within the membrane, with respect to their ability to conduct electron transport from water to Q_A. As shown in Table 1, the variable fluorescence yields for both mutant strains approximated those of the control strain, indicating that the mutant PSII centers are fully capable of oxidizing water. These results mirrored those previously obtained for the R320S strain (Table 1; Young, et al., 2002). It should be noted that the *psbC* deletion strain, which contains no functional PSII centers, did not give a fluorescence signal.

Although the R320K and R320D strains appear to assemble near control amounts of PSII centers that one might assume from the above data are functioning relatively normally, this

is not the case, particularly under chloride-limiting conditions. The susceptibility of the PSII centers to photoinactivation was assessed by exposing the cells to a high light intensity. The process of photoinactivation leads to a number of structural changes within the PSII complex. These events include the rapid turnover of the D1 protein and proteolysis of the D2 protein and CP43 (Nedbal et al., 1990; Mori and Yamamoto, 1992; Aro et al., 1993), with a resultant drop in oxygen-evolving activity. The results for the control strain (Table 2) showed no appreciable differences between the $t_{0.5}$ values for samples grown in complete or chloride-deficient media. When grown in complete media and subjected to photoinactivating light, the R320K strain exhibited a $t_{0.5}$ value similar to the control value. The calculated $t_{0.5}$ for photoinactivation for the R320D mutant was 1.4 times less than that of control cells, indicating that this mutant is more sensitive to photoinactivation than the control. This suggests that, in complete media, there is a defect in the stability of the R320D PSII complex, while no defect is apparent for the R320K strain under these conditions.

Photoinactivation experiments were also performed on strains grown under conditions of chloride depletion (Table 2). The results of these experiments indicate that, while $t_{0.5}$ value for the control strain remained essentially the same compared to its value in complete media, the PSII stability of both mutant strains was altered under these conditions. For the R320K strain grown in chloride-deficient media, the $t_{0.5}$ value was 2.9 min compared to 5.7 min for the control, indicating that this mutant is photoinactivating at twice the rate of the control under these conditions. Photoinactivation was difficult to measure in the R320D mutant due to its low rate of oxygen evolution. Given this, R320D cells demonstrated an extreme sensitivity to photoinhibition, with a calculated $t_{0.5}$ for photoinactivation 6 times less than that of the control. Thus, the PSII centers in all the mutants become destabilized under chloride-limiting conditions.

Comparison of the results of this photoinactivation study to those obtained for the R320S mutant (Table 2; Young et al., 2002) highlights some notable trends. The PSII stability of these strains seems to follow the following pattern in complete media: Control ≈ R320K > R320S > R320D. This trend is only slightly modified when the strains are grown in chloride-deficient media, and follows the pattern: Control > R320K ≈ R320S > R320D. When chloride is not limiting in the media, it appears that various amino acid substitutions can be made at this site with limited effect on the stability of PSII. However, the results also indicate that when chloride is limiting, even substitution of an amino acid with similar properties to arginine, such as lysine, is not sufficient to preserve the integrity of the interactions in which this site is involved.

In order to gain a better understanding of the effect of the mutations on possible interactions with cytochrome c_{550}, PSII core particles were isolated from His-tagged control and mutant strains using cobalt metal affinity chromatography. The effectiveness of this method for isolating active PSII particles has been documented (Bricker et al., 1998). Fig. 4 shows the optical absorption spectra obtained from the PSII particles derived from the control and two mutant strains. There are no apparent differences in the spectra, each of which shows a characteristic absorption maximum at 674 nm. Reduced minus oxidized difference spectra were obtained from the isolated control, R320K, and R320D His-tagged particles (Fig. 5). These indicated that while the control particles were able to retain cytochrome c_{550} within the particle, the mutant strains were not (Fig. 5). This was true whether the cells were grown in complete (Fig. 5) or chloride-deficient media (not shown). These results are similar to those obtained previously with the R320S mutant, which was unable to retain the

association between PSII and cytochrome c_{550} after purification of these particles, regardless of the media in which the cells were grown. Thus, even a conservative substitution (lysine) at this site, which results in a fairly functional mutant under normal growth conditions, prevents the strong association of cytochrome c_{550}. It is possible that some cytochrome c_{550} associates with these mutants in vivo, but that the relatively harsh conditions used to isolate the particles disrupt this interaction. We are currently probing the kinetics of binding of cytochrome c_{550} to His-tagged PSII from these strains in order to examine this.

8. Conclusion

Site-directed mutagenesis has been employed extensively to probe the function of the CP43 protein of PSII. In particular, substitutions at Arg320 have revealed a potential role of this amino acid in the interaction of CP43 with the extrinsic PSII protein, cytochrome c_{550}. In the present study, we have further defined the requirement at position 320 by constructing and characterizing additional mutant strains R320K and R320D. The results indicate that both the R320K and R320D strains are defective in their ability to utilize chloride to carry out efficient oxygen evolution and the effect is magnified under low chloride conditions. Spectrophotometrically detectable cytochrome c_{550} is lacking in these mutants. Additionally, we have preliminary evidence that these mutants also lack PsbU (Bricker and Putnam-Evans, unpublished). The phenotype of the R320S mutant previously described is intermediate between that of the K and D mutants. Thus, the order of effectiveness of amino acids at this site in supporting normal PSII function is R>K>S>D. A positively charged residue appears to be required at this site for proper function. The 1.9 Å crystal structure reveals a number of amino acid residues within both cytochrome c_{550} and PsbU that are potential hydrogen bonding partners to Arg320. Our operating hypothesis is that CP43, cytochrome c_{550} and PsbU interact via a hydrogen-bonding network that is involved in promoting a stable environment for chloride incorporation into the active site. While the position and ligands of chloride around the manganese cluster are now known, what other proteins bind chloride, how chloride is funneled to the active site, and where potential chloride channels occur remain unclear. Continuing studies to address these questions will no doubt expand our knowledge of the protein-protein and protein-ligand interactions in PSII that contribute to the proper functioning of the oxygen-evolving complex.

9. Acknowledgment

This work was supported by a U.S. National Science Foundation grant (MCB9982981) to CP-E, and a U.S. Department of Energy grant (DE-FG02-98ER20310) to TMB.

10. References

Ananyev G., Nguyen T., Putnam-Evans C., & Dismukes, C. (2005) Mutagenesis of CP43-arginine-357 to serine reveals new evidence for (bi)carbonate functioning in the water oxidizing complex of Photosystem II. *Photochemical and Photobiological Sciences*, Vol. 4, pp. 991–998.

Aro, E.-M., Virgin, I., & Andersson, B. (1993) Photoinhibition of photosystem II. Inactivation, protein damage and turnover. *Biochimica et Biophysica Acta*, Vol. 1143, pp. 113-134.

Bricker, T. (1990) The structure and function of CPa-1 and CPa-2 in photosystem II. *Photosynthesis. Research,* Vol. 24, pp. 1-13.

Bricker, T. (1992) Oxygen evolution in the absence of the 33 kDa manganese-stabilizing protein. *Biochemistry*, Vol. 31, pp. 4623-4628.

Bricker, T., Morvant, J., Masri, N., Sutton, H., & Frankel, L. (1998) Isolation of a highly active photosystem II preparation from Synechocystis 6803 using a histidine-tagged mutant of CP 47. *Biochimica et Biophysica Acta*, Vol. 1409, pp. 50-7.

Bricker, T., A. Young, L.K. Frankel, and C. Putnam-Evans. (2002) Introduction of the ^{305}Arg→ ^{305}Ser mutation in the large extrinsic loop E of the CP43 protein of Synechocystis sp. PCC 6803 leads to the loss of cytochrome c_{550} binding to photosystem II. *Biochimica et Biophysica Acta,* Vol. 1556, pp. 92-96.

Bricker, T. & Frankel, L. (2002) The structure and function of CP47 and CP43 in Photosystem II. *Photosynthesis Research*, Vol. 72, pp. 131-146.

Bricker, T., Roose, J., Fagerlund, R., Frankel, L., & Eaton-Rye, J. (2011) The extrinsinc proteins of photosystem II. *Biochimica et Biophysica Acta*, doi:10.1016/j.bbabio.2011.07.006 [Epub ahead of print].

Burnap, R., Qian, M., Shen, J.-R., Inoue, Y., & Sherman, L. (1994) Role of disulfide linkage and putative intermolecular binding residues in the stability and binding of the extrinsic manganese-stabilizing protein to the photosystem II reaction center. *Biochemistry,* Vol. *33*, pp. 13712-13718.

Burnap, R., Shen, J.-R., Jursinic, P., Inoue, Y., & Sherman, L. (1992) Oxygen yield and thermoluminescence characteristics of a cyanobacterium lacking the manganese-stabilizing protein of Photosystem II. *Biochemistry*, Vol. 31, pp. 7404–7410.

Carpenter, S., Charite, J., Eggars, B., & Vermaas, W. (1990) The psbC start codon in *Synechocystis* sp. PCC 6803. *FEBS Letters*, Vol. 1, pp. 135-137.

Chu, H.-A., Nguyen, A. & Debus, R. (1994) Site-directed photosystem II mutants with perturbed oxygen-evolving properties. 1. Instability or inefficient assembly of the manganese cluster in vivo. *Biochemistry*, Vol. 33, pp. 6137-6149.

Clarke, S., & Eaton-Rye, J. (1999) Mutation of Phe-363 in the Photosystem II protein CP 47 impairs photoautotrophic growth, alters the chloride requirement, and prevents photosynthesis in the absence of either PSII-O or PSII-V in *Synechocystis* sp. PCC 6803. *Biochemistry*, Vol. 38, pp. 2707-2715.

Dau, H., & Haumann, M. (2008) The manganese complex of photosystem II in its reactioncycle—basic framework and possible realization at the atomic level. *Coordination Chemistry Reviews*, Vol. 252, pp. 273–295.

Debus, R., Barry, B., Sithole, I., Babcock, G., & McIntosh, L. (1988a) Directed mutagenesis indicates that the donor to P680+ in photosystem II is tyr-161 of the D1 polypeptide. *Biochemistry*, Vol. 27, pp. 907-9074.

Debus, R., Barry, B., Babcock, G., & McIntosh, L. (1988b) Site-specific mutagenesis identifies a tyrosine radical involved in the photosynthetic oxygen-evolving complex. *Proceedings of the National Academy of Science* (USA), Vol. 85, pp. 427- 430.

Dzelzkalns, V., & Bogorad, L. (1988) Molecular analysis of a mutant defective in photosynthetic oxygen evolution and isolation of a complementing clone by a novel screening procedure. *EMBO Journal*, Vol. 7, pp. 333-338.

Ferreira, K., Iverson, T., Maghlaoui, K., Barber, J., & Iwata, S. (2004) Architecture of the photosynthetic oxygen-evolving center. *Science*, Vol. 303, pp.1831-8.

Gabdulkhakov, A., Guskov, A., Broser, M., Kern, J., Müh, F., Saenger, W., & Zouni, A. (2009) Probing the accessibility of the Mn4Ca cluster in Photosystem II; channels calculation, noble gas derivatization, and cocrystallization with DMSO. *Structure*, Vol. 17, pp. 1223–1234.

Ghanotakis, D., Topper, J., & Yocum, C. (1984) Structural organization of the oxidizing side of photosystem II: exogenous reductants reduce and destroy the Mn complex in photosystem II membranes depleted of the 17 and 23 kDa polypeptides. *Biochimica et Biophysica Acta*, Vol. 767, pp. 524–531.

Ghanotakis, D., Babcock, G., & Yocum, C. (1985) On the role of water-soluble polypeptides (17, 23 kDa) calcium and chloride in photosynthetic oxygen evolution. *FEBS Letters*, Vol. 192, pp. 1–3.

Glazer, A. (1983) Comparative biochemistry of photosynthetic light-harvesting systems. *Annual Review of Biochemistry*, Vol. 52, pp.125-157.

Grabolle, M., Haumann, M., Müller, C., Liebisch, P. & Dau, H. (2006) Rapid loss of structural motifs in the manganese complex of oxygenic photosynthesis by Xray irradiation at 10–300 K. *Journal of Biological Chemistry*, Vol. 281, pp. 4580–4588.

Hwang, H., Dilbeck, P., Debus, R., & Burnap, R. (2007) Mutation of arginine 357 of the CP43 protein of photosystem II severely impairs the catalytic S-state cycle of the H2O oxidation complex. *Biochemistry*, Vol. 46, pp. 11987–11997.

Inoue-Kashino, N., Kashino, Y., Satoh, K., Terashima, I., & Pakrasi, H. (2005) PsbU provides a stable architecture for the oxygen-evolving system in cyanobacterial Photosystem II. *Biochemistry*, Vol. 44, pp. 12214–12228.

Joliot, P., Barbieri, G. & Cjabaud, R. (1969) Un nouveau modele des centres photochemiques du systeme II. *Photochemistry and Photobiology*, Vol.10, pp. 309-329.

Kamiya, N. & Shen, J.-R. (2003) Crystal structure of oxygen-evolving photosystem II from Thermosynechococcus vulcanus at 3.7-Å resolution. *Proceedings of the National Academy of Science* (USA), Vol. 100, pp. 98-103.

Katoh, H., Itoh, S., Shen, J.-R., & Ikeuchi, M. (2001) Functional analysis of psbVand a novel c-type cytochrome gene psbV2 of the thermophilic cyanobacterium Thermosynechococcus elongatus Strain BP-1. *Plant Cell Physiology*, Vol. 42, pp. 599–607.

Kawakami, K., Umena, Y., Kamiya, N., & Shen, J-R. (2011) Structure of the catalytic, inorganic core of oxygen-evolving photosystem II at 1.9 Å resolution. *Journal of Photochemistry and Photobiology B*, Vol. 104, pp. 9-18.

Kelley, P., & Izawa, S. (1978) The role of chloride ion in photosystem II. I. Effects of chloride ion on photosystem II electron transport and on hydroxylamine inhibition. *Biochimica et Biophysica* Acta, Vol. 502, pp. 198-210.

Klimov, V., Dolan, E. & Ke, B. (1980) EPR properties of an intermediary electron acceptor (pheophytin) in photosystem II reaction centers at cryogenic temperatures. *FEBS Letters*, Vol. 112, pp. 97-100.

Knoepfle, N., Bricker, T., & Putnam-Evans, C. (1999) Site-directed mutagenesis of basic arginine residues 305 and 342 in the CP 43 protein of photosystem II affects oxygen-evolving activity in Synechocystis 6803. *Biochemistry*, Vol. 38, pp. 1582-1588.

Kok, B., Forbush, B. & McGloin, M. (1970) Cooperation of charges in photosystem II O_2 evolution I: A linear 4-step model. *Photochemistry and Photobiology*, Vol. 11, pp. 457-475.

Kuhn, M., & Vermaas, W. (1993) Deletion mutations in a long hydrophilic loop in the photosystem II chlorophyll-binding protein CP43 in the cyanobacterium *Synechocystis* sp. PCC 6803. *Plant Molecular Biology*, Vol. 23, pp. 123-133.

Kuwabara, T., Miyao, M., Murata, T., & Murata, N. (1985) The function of the 33 kDa protein in the oxygen evolution system studied by reconstitution experiments. *Biochimica et Biophysica* Acta, Vol. 806, pp. 283-289.

Liu, H., Frankel, L., & Bricker, T. (2007) Functional analysis of Photosystem II in a PsbO-1 deficient mutant in Arabidopsis thaliana. *Biochemistry,* Vol. 46, pp. 7607–7613.

McEvoy, J., & Brudvig, G. (2006) Water-splitting chemistry of photosystem II. *Chemical Reviews*, Vol. 106, pp. 4455-4483.

Miyao, M., Murata, N., Lavorel, J., Maison-Peteri, B., Boussac, A., & Etienne, A-L. (1987) Effect of the 33-kDa protein on the S-state transitions in photosynthetic oxygen evolution. *Biochimica et Biophysica Acta*, Vol. 890, pp. 151–159.

Mori, H., & Yamamoto, Y. (1992). Deletion of antenna chlorophyll-a-binding proteins CP43 and CP47 by tris-treatment of PS II membranes in weak light: Evidence for a photo-degradative effect on the PS II components other than the eaction center-binding proteins. *Biochimica et Biophysica Acta*, Vol. 1100, pp. 293-298.

Nedbal, L., Masojídek, J., Komenda, J., Prášil, O., &. Šetlík, I. (1990). Three types of PSII photoinactivation. 2. Slow processes. *Photosynthesis. Research*, Vol. 24, pp. 89-97.

Nixon, P., & Diner, B. (1992) Aspartate 170 of the photosystem II reaction center polypeptide D1 is involved in the assembly of the oxygen-evolving manganese cluster. *Biochemistry*, Vol. 31, pp. 942-948.

Noren, G., Boerner, R., & Barry, B. (1991) EPR characterization of an oxygen-evolving photosystem II preparation from the transformable cyanobacterium Synechocystis 6803. *Biochemistry*, Vol. 30, pp. 3943–3950.

Ono, T., & Inoue, Y. (1984) Reconstitution of photosynthetic oxygen-evolving activity by rebinding of 33 kDa protein to $CaCl_2$-extracted PS II particles. *FEBS Letters*, Vol. 166, pp. 381–384.

Popelkova, H., & Yocum, C. (2007) Current status of the role of Cl− ion in the oxygen-evolving complex. *Photosynthesis Research*, Vol. 93, pp. 111–121.

Putnam-Evans, C. & Bricker, T. (1994) Site-directed mutagenesis of the Cpa-1 protein of Photosystem II:alteration of the basic residue ^{448}Arg to ^{448}Gly prevents the stable assembly of functional Photosystem II centers under chloride-limiting conditions. *Biochemistry*, Vol. 33, pp. 10770-10776.

Putnam-Evans , C., & Bricker T. (1997) Site-directed mutagenesis of the basic residues 321K to 321G in the CP 47 protein of photosystem II alters the chloride requirement for growth and oxygen-evolving activity in Synechocystis 6803. *Plant Molecular Biology*, Vol. 34, pp. 455-63.

Renger, G., & Renger, T. (2008) Photosystem II: the machinery of photosynthetic water splitting. *Photosynthesis Research*, Vol. 98, pp. 53–812.

Rochaix, J.-D., Kuchka, M., Mayfield, S., Schirmer-Rahire, M., Girard-Bascou, J., & Bennoun, P. (1989) Nuclear and choroplast mutations affect the synthesis or stability of the chloroplast psbC gene product in *Chlamydomonas reinhardtii*. *EMBO Journal*, Vol. 8, pp. 1013-1021.

Rogner, M., Chisholm, D. & Diner, B. (1991) Site-directed mutagenesis of the *psb*C gene of photosystem II: isolation and functional characterization of CP43-less photosystem II core complexes. *Biochemistry,* Vol. 30, pp. 5387-5395.

Roose, J., Kashino, Y., & Pakrasi, H. (2007) The PsbQ protein defines cyanobacterial Photosystem II complexes with highest activity and stability. *Proceedings of the National Academy of Science* (USA), Vol. 104, pp. 2548-2553.

Rosenberg, C., Christian, J., Bricker, T., & Putnam-Evans, C. (1999) Site-directed mutagenesis of glutamate residues in the large extrinsic loop of the Photosystem II protein CP 43 affects oxygen-evolving activity and PSII assembly. *Biochemistry*, Vol. 38, pp. 15994-16000.

Sandusky, P., & Yocum, C. (1983) The mechanism of amine inhibition of the photosynthetic oxygen-evolving complex: amines displace functional chloride from a ligand site on manganese. *FEBS Letters*, Vol 162, pp. 339–343.

Sayre, R., & Wrobelboerner, E. (1994) Molecular topology of the Photosystem II chlorophyll alpha binding protein, CP43:topology of a thylakoid membrane protein. *Photosynthesis Research,* Vol. 40, pp. 11-19.

Service, R., Yano, J., McConnell, I., Hwang, H., Niks, D., Hille, R., Wydrzynski, T., Burnap, R., Hillier, W., & Debus, R. (2011) Participation of glutamate-354 of the CP43 polypeptide in the ligation of manganese and the binding of substrate water in photosystem II. *Biochemistry*, Vol. 50, pp. 63-81.

Shen, G., Eaton-Rye, J., & Vermaas, W. (1993) Mutation of histidine residues in CP47 leads to a destabilization of the photosystem II complex and to impairment of light energy transfer. *Biochemistry*, Vol. 32, pp. 5109-5115.

Shen, J.-R., Burnap, R., & Inoue, Y. (1995) An independent role of cytochrome c-550 in cyanobacterial Photosystem II as revealed by double-deletion mutagenesis of the psbO and psbV genes in Synechocystis sp. PCC 6803. *Biochemistry*, Vol. 34, pp. 12661–12668.

Shen, J.-R., Ikeuchi, M., & Inoue, Y. (1997) Analysis of the psbU gene encoding the 12-kDa extrinsic protein of Photosystem II and studies on its role by deletion mutagenesis in Synechocystis sp. PCC 6803. *Journal of Biological Chemistry*, Vol. 272 , pp. 17821–17826.

Shen, J.-R. Qian, M., Inoue, Y., & Burnap, R. (1998) Functional characterization of Synechocystis sp. PCC 6803 ΔpsbU and ΔpsbV mutants reveals important roles of

cytochrome c-550 in cyanobacterial oxygen evolution. *Biochemistry*, Vol. 37, pp. 1551–1558.

Shimada, Y., Suzuki, H., Tsuchiya, T., Tomo, T., Noguchi, T., & Mimuro, M. (2009) Effect of a single-amino acid substitution of the 43 kDa chlorophyll protein on the oxygen-evolving reaction of the cyanobacterium Synechocystis sp. PCC 6803: analysis of the Glu354Gln mutation. *Biochemistry*, Vol. 48, pp. 6095-103.

Shimada, Y., Suzuki, H., Tsuchiya, T., Mimuro, M., & Noguchi, T. (2011) Structural coupling of an arginine side chain with the oxygen-evolving Mn4Ca cluster in photosystem II as revealed by isotope-edited Fourier transform infrared spectroscopy. *Journal of the American Chemical Society*, Vol. 133, pp. 3808-11.

Strickler, M., Hwang, H., Burnap, R., Junko, Y., Walker, L., Service, R., Britt, D., Hillier, W., & Debus, R. (2008) Glutamate- 354 of the CP43 polypeptide interacts with the oxygen-evolving Mn4Ca cluster of photosystem II: a preliminary characterization of the Glu354Gln mutant. *Philosophical Transactions of the Royal Society B,* Vol. 363, pp. 1179- 1188.

Tang, X.-S., & Diner, B. (1994) Biochemical and spectroscopic characterization of a new oxygen-evolving photosystem II core complex from the cyanobacterium Synechocystis PCC 6803. *Biochemistry*, Vol. *33*, pp 4594–4603.

Umena, Y., Kawakami, K., Shen, J-R., & Kamiya, N. (2011) Crystal structure of oxygen-evolving photosystem II at a resolution of 1.9 Å. *Nature*, Vol. 473, pp. 55-60.

Vassiliev, S., Comte, P., Mahboob, A., & Bruce, D. (2010) Tracking the flow of water through photosystem II using molecular dynamics and streamline tracing. *Biochemistry*, Vol. 49, pp. 1873–1881.

Vermaas, W., Rutherford, A., & Hansson, O. (1988) Site directed mutagenesis in photosystem II of the cyanobacterium *Synechocystis* sp. PCC 6803: Donor D is a tyrosine residue in the D2 protein. *Proceedings of the National Academy of Science (USA)*, Vol. 85, pp. 8477-8481.

von Heijne, G., & Gavel, Y. (1988) Topologenic signals in integral membrane proteins. *European Journal of Biochemistry,* Vol. 174, pp. 671-678.

Williams, J. (1988) Construction of specific mutations in photosystem II reaction center by genetic engineering methods in *Synechocystis* 6803. *Methods in Enzymology*, Vol. 167, pp. 766-778.

Wincencjusz, H., van Gorkom, H., & Yocum, C. (1997) The photosynthetic oxygen-evolving complex requires chloride for its redox state S2→S3 and S3→S0 transitions but not for S0→S1 or S1→S2 transitions. *Biochemistry*, Vol. 36, pp. 3663- 3670.

Yachandra, V., DeRose, V., Latimer, M., Mukerji, I., Sauer, K., & Klein, M. (1993) A structural model for the photosynthetic oxygen-evolving manganese complex. *Japanese Journal of Applied Physics*, Vol. *32s*, 523-526.

Young, A., McChargue, M., Frankel, L., Bricker, T. & Putnam-Evans, C. (2002) Alterations of the oxygen-evolving apparatus induced by a 305Arg → 305Ser mutation in the CP42 protein of photosystem II from Synechocystis sp. PCC 6803 under chloride-limiting conditions. *Biochemistry*, Vol. 41, pp. 15747-15753.

Zouni, A., Witt, H., Kern, J., Fromme, P., Krauss, N., Saenger, W. & Orth., P. (2001) Crystal structure of photosystem II from *Synechococcus elongatus* at 3.8 Å resolution. *Nature*, Vol. 409, pp. 739-743.

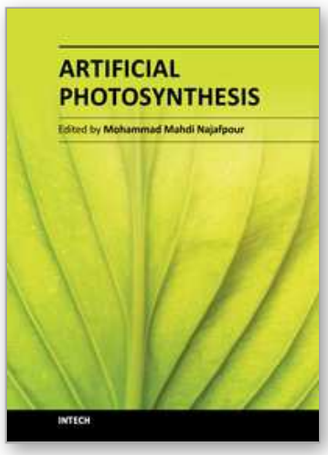

Artificial Photosynthesis

Edited by Dr Mohammad Najafpour

ISBN 978-953-307-966-0
Hard cover, 288 pages
Publisher InTech
Published online 24, February, 2012
Published in print edition February, 2012

Photosynthesis is one of the most important reactions on Earth, and it is a scientific field that is intrinsically interdisciplinary, with many research groups examining it. We could learn many strategies from photosynthesis and can apply these strategies in artificial photosynthesis. Artificial photosynthesis is a research field that attempts to replicate the natural process of photosynthesis. The goal of artificial photosynthesis is to use the energy of the sun to make different useful material or high-energy chemicals for energy production. This book is aimed at providing fundamental and applied aspects of artificial photosynthesis. In each section, important topics in the subject are discussed and reviewed by experts.

InTech Europe
University Campus STeP Ri
Slavka Krautzeka 83/A
51000 Rijeka, Croatia
Phone: +385 (51) 770 447
Fax: +385 (51) 686 166
www.intechopen.com

InTech China
Unit 405, Office Block, Hotel Equatorial Shanghai
No.65, Yan An Road (West), Shanghai, 200040, China
中国上海市延安西路65号上海国际贵都大饭店办公楼405单元
Phone: +86-21-62489820
Fax: +86-21-62489821

IntechOpen